Maximal and submaximal isometric torque is elevated immediately following highly controlled active stretches of the hamstrings

Neil Chapman [a,*], John Whitting [a], Suzanne Broadbent [b], Zachary Crowley-McHattan [a], Rudi Meir [a]

[a] *Southern Cross University, Lismore, NSW, Australia*
[b] *University of the Sunshine Coast, Sippy Downs, Queensland, Australia*

ARTICLE INFO

ABSTRACT

Hamstring strain rehabilitation programs with an eccentric bias are effective but have a low adherence rate. Post-stretch isometric (PS-ISO) contractions which incorporate a highly controlled eccentric contraction followed by an isometric contraction resulting in elevated torque during following stretch, compared with isometric contractions at the same joint angle. This study measured torque, activation and musculotendinous unit behaviour of the hamstrings during PS-ISO contractions of maximal and submaximal levels using two stretch amplitudes. Ten male participants (24.6 years $\pm$ 2.22 years) completed maximal and submaximal baseline isometric contractions at 90°, 120° and 150° knee flexion and PS-ISO contractions of maximal and submaximal intensity initiated at 90° and 120° incorporating active stretch of 30° and 60° at 60°·s^{-1}. Torque and muscle activation of the knee flexors were simultaneously recorded. Musculotendinous unit behaviour of the biceps femoris long head was recorded via ultrasound during all PS-ISO contractions. Compared with baseline, torque was 8% and 39% greater in the maximal and submaximal PS-ISO conditions respectively with no change in muscle activation. The biceps femoris long head muscle lengthened during all PS-ISO contractions. PS-ISO contractions may be beneficial where the effects of highly controlled eccentric contractions and elevated isometric torque are desired, such as hamstring rehabilitation.

1. Introduction

Despite considerable interest in injury prevention and rehabilitation strategies, the incidence and recurrence of hamstring strain injuries remains high (Brooks et al., 2006). The biceps femoris long-head (BF*lh*) is the most commonly injured of the hamstring muscle group (Gibbs et al., 2004), and high-speed running, one of the most common injury mechanisms (Gabbe et al., 2006). A lack of isometric strength leading to a force eccentric lengthening during the late swing phase of high-speed running, or braking during the late swing phase of high-speed running are proposed as potential causes of injury (Van Hooren and Bosch, 2017a, Van Hooren and Bosch, 2017b). Rehabilitation of hamstring injuries typically focusses on; i) minimisation of scar tissue formation and subsequent reduction in musculotendinous unit extensibility (Proske et al., 2004), ii) the restoration of isometric and eccentric strength (Hickey et al., 2020, Van Hooren and Bosch, 2017a, Van Hooren and Bosch, 2017b) and iii) the correction of altered

neuromuscular control following injury (Erickson and Sherry, 2017). It has also been proposed that rehabilitation program should address psychosocial factors, such as apprehension and fear of movement when completing ballistic tasks (Askling et al., 2010). However, consensus is lacking regarding best practice in hamstring injury rehabilitation (Comfort et al., 2009), which may explain lengthy recovery times typically experienced by athletes (Orchard and Best, 2002).

Eccentric strength training such as the L-protocol (Askling et al., 2014) and the Nordic hamstring exercise (Brockett et al., 2001) are commonly used in rehabilitation. Strength training with an eccentric bias has been shown to offset the effects of scar tissue (Proske et al., 2004), increase in series compliance resulting in a rightward shift in the length-tension curve (Tyler et al., 2015). However, despite the evidence for effectiveness, negative perceptions persist that eccentric exercise increases pain and thus adherence to eccentric exercise remains sub-par (van der Horst et al., 2020). This perception is potentially re-enforced by conventional guidelines which recommend the avoidance of pain during
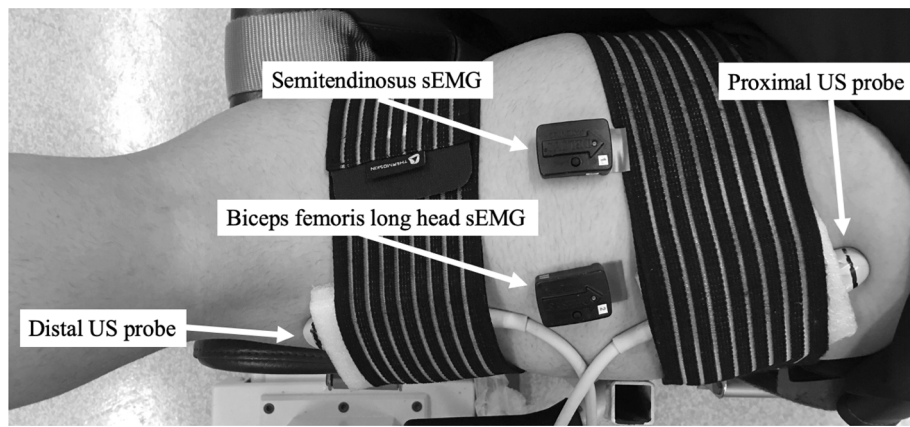

Fig. 1. The participant was positioned lying prone on the dynamometer. The positions of the proximal and distal ultrasound probes and the sEMG sensors position on BF*lh* and Semitendinosus are pictured.

the treatment of acute muscle injuries (Järvinen et al., 2005). Notwithstanding this, these conventional guidelines concede that the current treatment principles lack scientific basis (Järvinen et al., 2005). Nonetheless, this contradictory approach may influence the exercise selection of some practitioners towards more conservative contraction modes such as isometric contractions (Heiderscheit et al., 2010). In contrast, isometric contractions are often favoured in early-stage rehabilitation and are advocated to be at least as effective as eccentric contractions (Van Hooren and Bosch, 2017b). There may be favourable outcomes in combining eccentric and isometric contractions by harnessing the benefits of history dependence of muscle. It is also feasible that having greater control over the intensity and angular velocity of eccentric contractions may prove to be a more palatable approach where adherence to eccentric training is sub-par (van der Horst et al., 2020).

A potential option is the post-stretch isometric (PS-ISO) contraction. A PS-ISO contraction is initiated with an isometric contraction at a shorter muscle length, immediately followed by a highly controlled eccentric contraction, then a final isometric contraction at the new longer muscle length. *In vitro* evidence indicates that torque spikes sharply during the eccentric phase of the PS-ISO, before normalising somewhat, however remains elevated during the PS-ISO steady state contraction. The PS-ISO steady-state torque exceeds the predicted isometric torque at the corresponding muscle length without prior stretch, termed residual force enhancement (rFE) (Edman et al., 1982). It is theorised that the enhanced force is due to the giant protein titin increasing stiffness during stretch and maintained during the steady-state isometric contraction following stretch (Herzog and Leonard, 2005). Importantly, the enhanced force is observed in the absence of increased muscle activation (Herzog and Leonard, 2005). The magnitude of rFE is greatest at long muscle lengths and increases with increasing stretch amplitude (Herzog and Leonard, 2005), though is independent of stretch velocity (Lee and Herzog, 2002). Although in vitro evidence of rFE continues to build, to date, a single *in vivo* investigation has been undertaken which reported rFE of 4–5% in the hamstrings muscle group using maximal PS-ISO contractions (Shim and Garner, 2012). The magnitude of rFE *in vivo* has been shown to range from 3% to 25% in other lower limb muscles during maximal and submaximal voluntary contractions (Chen and Power, 2019). No study has, as yet, investigated rFE in the hamstrings muscle group using activation-matched submaximal PS-ISO contractions which are more relevant in rehabilitation.

The evidence for the use of eccentric stimulus in rehabilitation continues to mount, yet the effects of using a combined eccentric and isometric contraction mode which is highly controlled are as yet, unknown. Seiberl et al. (2015) have suggested that the phenomenon of rFE may be applicable in instances where high levels of force are required, particularly when the neuromuscular system is weakened. Therefore,

investigation of the acute effects of PS-ISO contractions of the hamstrings group is warranted. This study aimed to observe the presence of rFE using highly controlled maximal and submaximal PS-ISO contractions using two stretch amplitudes. The study also aimed to observe musculotendinous unit behaviour during the joint rotation of the PS-ISO contraction. It was hypothesised that rFE would be observed during all maximal and submaximal PS-ISO contractions without increased muscle activation. Secondly, it was hypothesised that BF*lh* muscle would lengthen, confirming an eccentric contraction, during the joint rotation of maximal and submaximal PS-ISO contractions using two stretch amplitudes.

2. Methods

2.1. Participants

Prior to recruitment, an a priori calculation calculated (n = 8). Ten physically active male participants (24.6 years ± 2.22 years) provided written informed consent to participate in the study. All participants were free from diagnosed lower limb musculoskeletal injury and neurologic conditions in the preceding 12 weeks. The study was approved by the Institutional Human Research Ethics Committee (ECN: 2019/090).

2.2. Experimental set-up

Participants were asked to assume a prone position on a Biodex System 3 dynamometer (Biodex Medical Systems, Shirley, NY; accuracy ± 7 Nm, resolution ± 0.02 Nm), which recorded torque measurements for all experiments. The axis of rotation of the right knee was aligned with the axis of rotation of the dynamometer. The ankle cuff was attached 25 mm above the dorsal surface of the foot. Inelastic straps were placed over the L4/5 area to mitigate extraneous movements of the trunk during contractions (Fig. 1). A manual goniometer (J.A. Preston Corporation, Clifton, NJ) was used to confirm that each participant's hip angle was set between to be between 170° and 180° (180° representing neutral hip position). The goniometer was centred on the greater trochanter of the right hip and aligned with the lateral midline of the abdomen and lateral midline of the femur.

Surface electromyography (sEMG) signals of BF*lh* and semitendinosus were recorded during all trials using a Trigno Wireless sEMG system with double differentiated surface electrodes (Delsys, Natick, MA, USA). Electrodes were placed, and sites prepared per SENIAM guidelines (Hermens et al., 1999).

Distal and proximal musculotendinous junctions were observed via B-mode ultrasound (MicrUS EXT-1H, Telemed Vilnius, Lithuania) using a dual-head linear transducer (frequency, 12 Hz; depth, 8 cm; field of
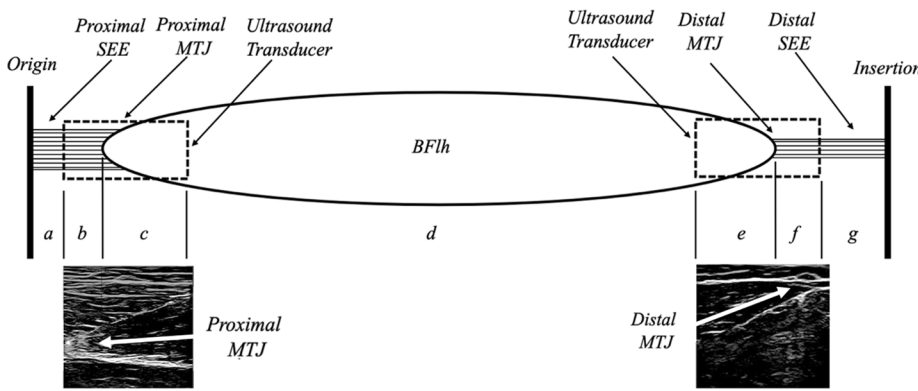
Fig. 2. Schematic of the ultrasound transducer positioning over the BFlh MTU and of the lengths used to calculate positional change of the CE and proximal and distal SEE. a = muscle origin to proximal edge of the proximal transducer, b = proximal edge of the proximal transducer to proximal MTJ, c = proximal MTJ to distal edge of the proximal transducer, d = distal edge of the proximal ultrasound transducer to the proximal edge of the distal transducer, e = proximal edge of the distal transducer to distal MTJ, f = distal MTJ to distal edge of distal transducer, g = distal edge of distal transducer to muscle insertion.

view, 12 × 70 mm). Each transducer was located over the proximal and distal musculotendinous junctions of BF*lh* respectively and aligned parallel with the direction of the muscle fibres. Transducers were firmly fixed to the leg using two custom-built Styrofoam housings (Fig. 1) and secured in place with elastic bandages (Tilp et al., 2011). A GoPro (GoPro Hero 7 Black, GoPro Inc, San Mateo, CA, USA), positioned directly above the participant's right leg recorded video images of the position of each ultrasound probe. B-mode ultrasound was chosen for its reproducibility (Kwah et al., 2013), high intra-class correlation coefficients (0.99) (Aeles et al., 2017) and suitability to study dynamic muscle changes (Franchi et al., 2018). As conventional B-mode ultrasound presents field of view limitations when viewing BF*lh* fascicles (Franchi et al., 2018), the investigators chose to observe and calculate the positional change of individual musculotendinous junctions during PS-ISO contractions to confirm whole muscle and tendon length change.

The sEMG signals were sampled at 2000 Hz (bandpass filtered at 10–500 Hz). Biodex data were sampled at 1000 Hz using a 12-bit analogue to digital converter (PowerLab System 16/35, ADInstruments, Bella Vista, Australia). Ultrasound video images were visualised using Echo Wave II software (Telemed Vilnius, Lithuania). GoPro video images were recorded at 1080p, 60fps. Biodex, sEMG, ultrasound and GoPro data were synchronised with LabChart software (Pro Modules 2014, version 8, ADInstruments, Bella Vista, Australia). Tracker software (Tracker Version 5.1.5) was used to plot and measure the positional change (in mm) of each musculotendinous junction during PS-ISO contractions in the ultrasound video images.

2.3. Experimental procedures

Following a 5-minute warmup on a cycle ergometer, participants performed three baseline maximal voluntary isometric contractions (MVIC), and three baseline activation matched voluntary isometric contractions of the knee flexors (5 s duration); the latter was performed

baseline trials (50% of MVIC), a matching target was calculated from this MVIC epoch with a ± 5% tolerance. The 50% activation matched trace was visualised on a computer monitor positioned within direct sight of participants.

Participants performed three maximal and three submaximal activation matched PS-ISO contractions of the knee flexors at 90° knee flexion (60° stretch amplitude) and at 120° knee flexion, (30° stretch amplitude) respectively (PS-ISO$_{MAX-long}$, PS-ISO$_{SUB-long}$, PS-ISO$_{MAX-short}$ and PS-ISO$_{SUB-short}$). A total of 12 experimental contractions. All active stretches occurred at a constant angular velocity of $60°.s^{-1}$ and were voluntarily activated for a total of 7 s, or 6.5 s respectively for the 60° and 30° joint excursions respectively. Participants were verbally encouraged to produce maximal effort during all maximal experimental conditions, and to closely match the activation matching target during all submaximal experimental conditions. Each participant could view either a torque trace (PS-ISO$_{MAX}$) or semitendinosus sEMG$_{RMS}$ trace (PS-ISO$_{SUB}$) on a television monitor located in their direct line of sight for visual feedback. Participants rested for 90 s between trials and 5 min between each experimental condition.

2.4. Data analysis

Mean torque (Nm) was derived from a 3 s epoch corresponding to 3–5 s for each baseline isometric and PS-ISO steady state experimental trial. Net torque (Nm) was averaged across contractions for each contraction condition in each participant. Mean sEMG$_{RMS}$ (mV) was derived from a 3 s epoch corresponding to 3–5 s for each experimental trial. The mean of the three experimental trials in each condition was used as the overall participant mean value. The rFE magnitude was defined as the absolute torque increase (Nm) and as a percentage change from the baseline MVIC and baseline 50% MVIA at 150°. The following equation was used to calculate percentage change rFE (Dalton et al., 2018):

$$rFE\%\Delta = [\frac{(Isometric\ torque\ N\hat{A}{\cdot}m\ following\ active\ lengthening - reference\ MVIC\ N\hat{A}{\cdot}m)}{Reference\ MVIC\ N\hat{A}{\cdot}m}] \times 100\%$$

at three knee joint angles (90°, 120°, and 150° knee position, 180° representing full knee extension). Participants rested for 90 s after each maximal or activation matched trial, with an additional 5 min rest between maximal and submaximal baseline trials. The activation matched baseline was calculated using the activation of the semitendinosus muscle. The mean of the root mean square (RMS) amplitude (mV) of the sEMG (sEMG$_{RMS}$: moving average window = 50 ms) was derived from a 3 s epoch, corresponding to seconds 2–4 in the MVIC baseline contractions. To standardise activation levels during activation matched

For MTU length change measurements, the positions of origin, insertion and ultrasound transducers located over the proximal and distal musculotendinous junctions with the knee flexed at 90°, 120°, and 150° were determined by direct measurement (mm) at the time of data collection (Fig. 2). Direct measurements were later confirmed by using the GoPro video images which were visualised and measured (mm) using Tracker software. A series of ultrasound images (image sequence recordings) were used to determine musculotendinous junction positional change during PS-ISO contractions in each PS-ISO contraction.

Table 1
Torque and sEMG$_{RMS}$ during maximal and submaximal baseline isometric and PS-ISO contractions of biceps femoris long-head (BFlh) and semitendinosus (ST).

	Torque (Nm)			BFlh (mV)			ST (mV)		
	M	SD	SE	M	SD	SE	M	SD	SE
Baseline Max	190.33	39.35	12.44	0.14	0.04	0.01	0.16	0.04	0.01
PS-ISO$_{MAX-long}$	196.91	32.01	10.12	0.12	0.03	0.01	0.16	0.06	0.02
PS-ISO$_{MAX-short}$	**207.34**	31.46	9.95	0.12	0.04	0.01	0.14	0.05	0.02
Baseline Sub	58.52	12.54	3.97	0.06	0.02	<0.00	0.08	0.02	<0.00
PS-ISO$_{SUB-long}$	**81.58**	19.33	6.11	0.06	0.02	<0.00	0.08	0.02	<0.00
PS-ISO$_{SUB-short}$	**81.35***	13.00	4.11	0.06	0.02	<0.00	0.08	0.02	<0.00

Mean values (M), standard deviation (SD) and standard error (SE) presented for baseline isometric contractions and PS-ISO contractions. Bold values indicate significant differences ($p < 0.05$), additional asterisk indicate highly significant (*$p < 0.001$) differences between baseline and PS-ISO contractions.

Table 2
Measurements of muscle, distal tendon and proximal tendon prior to and following PS-ISO with 30° (short) and 60° (long) joint rotations.

	Distal Tendon (mm)			Muscle (mm)			Proximal Tendon (mm)		
	M	SD	SE	M	SD	SE	M	SD	SE
Pre-Stretch short	41.33	5.89	1.86	312.84	7.27	2.29	48.32	5.02	1.59
PS-ISO$_{MAX-short}$	**47.44***	7.18	2.72	**327.38****	7.98	2.52	**38.72****	6.84	2.16
PS-ISO$_{SUB-short}$	**48.07**	7.67	2.43	**324.19***	9.41	2.97	**41.28***	7.26	2.29
Pre-Stretch long	41.93	6.64	2.10	317.57	11.06	3.50	42.95	6.74	2.13
PS-ISO$_{MAX-long}$	**56.46****	7.59	2.40	**329.18***	7.66	2.42	**38.02***	6.77	2.14
PS-ISO$_{SUB-long}$	**56.82****	5.71	1.81	**329.91****	9.45	2.99	**38.58**	6.62	2.09

Mean values (M), standard deviation (SD) and standard error (SE) presented for baseline isometric contractions and PS-ISO contractions. Bold values indicate significant differences ($p < 0.05$), additional asterisks highly significant differences (*$p < 0.01$; **$p < 0.001$) in length between pre-stretch and following PS-ISO contractions.

This technique was adapted from Aeles et al. (2017) who noted an average intra-rater ICC of 0.857 and SEM of 2.59 mm ± 1.56 mm. Positional measurements are illustrated in Fig. 2. Intra-rater reliability was established for the ultrasound measurements using Cronbach's alpha; (CE = 0.980, proximal tendon = 0.995, and distal tendon = 0.982).

The length of the muscle, proximal series elastic element and distal series elastic element were calculated via the equations below;

Muscle length = c + d + e
Proximal series elastic element length = a + b
Distal series elastic element length = f + g

To calculate the change in length of the muscle, proximal series elastic element and distal series elastic element during the active stretch phase of the PS-ISO contraction, the post-stretch lengths (150° knee flexion) were subtracted from the pre-stretch lengths (either 90° or 120° knee flexion).

All variables of interest were tested using the Shapiro-Wilk tests and found to be normally distributed. A repeated measures ANOVA was performed to calculate the differences in; torque, sEMG$_{RMS}$ of BFlh and semitendinosus and muscle and tendon length between the baseline isometric contraction at 150° knee flexion and PS-ISO steady state at 150° knee flexion. These calculations were made for all experimental conditions, maximal and submaximal activation matched conditions. Effect sizes were calculated using partial eta squared (0.20 = small, 0.50 = medium, 0.80 = large effect size) (Cohen, 2013). Significance was determined based on an $\alpha = 0.05$. Descriptive data in text and figures are reported as mean and standard deviation ($\pm$SD).

3. Results

3.1. Torque

A significant rFE was observed across maximal ($p = 0.013$, $\eta^2 = 0.381$) and submaximal rFE conditions ($p = 0.001$, $\eta^2 = 0.663$). No difference in torque was observed between joint rotations of maximal ($p = 0.056$) and submaximal ($p = 1.000$) conditions. All torque measurements and pairwise comparisons are presented in Table 1.

3.2. sEMG$_{RMS}$

A significant difference was observed in the maximal BFlh sEMG$_{RMS}$ increased from baseline to PS-ISO condition ($p = 0.023$, $\eta^2 = 0.342$). There was no difference in submaximal sEMG$_{RMS}$ from baseline to PS-ISO conditions of BFlh ($p = 0.957$, $\eta^2 = 0.005$) and semitendinosus ($p = 0.755$, $\eta^2 = 0.031$). There was no difference in maximal semitendinosus sEMG$_{RMS}$ from baseline to PS-ISO condition ($p = 0.346$, $\eta^2 = 0.111$). All sEMG$_{RMS}$ measurements including pairwise comparisons are presented in Table 1.

3.3. Muscle and tendon length

During all PS-ISO contractions, the muscle (60° joint rotation $p = <0.001$, $\eta^2 = 0.752$; 30° joint rotation $p = <0.001$, $\eta^2 = 0.710$) and distal tendon (60° joint rotation $p = <0.001$, $\eta^2 = 0.839$; 30° joint rotation $p = 0.001$, $\eta^2 = 0.561$) lengthened. The proximal tendon shortened during all PS-ISO contractions (60° joint rotation $p = 0.001$, $\eta^2 = 0.831$; 30° joint rotation $p = 0.001$, $\eta^2 = 0.815$). All whole muscle and tendon measurements and pairwise comparisons are presented in Table 2.

4. Discussion

This study confirmed rFE during maximal and submaximal PS-ISO contractions without increased muscle activation in the hamstrings muscle group. Lengthening of the BFlh muscle was confirmed during the eccentric portion of the PS-ISO contractions. As such, both hypotheses were confirmed. The magnitude of rFE in the PS-ISO$_{MAX-short}$ condition (8.94%) was greater than the only other investigation of the hamstrings muscle group (4–5%) (Shim and Garner, 2012). The observed rFE in PS-ISO$_{SUB-long}$ and PS-ISO$_{SUB-short}$ conditions (39%) are the first to be recorded in the hamstrings muscle group and is greater than previous studies of submaximal intensity using other lower limb muscles (25%) (Chen and Power, 2019). It is highly likely that altered titin stiffness during muscle stretch contributed to the elevated PS-ISO steady-state force. However, due to the complexity of the in-vivo model used in this
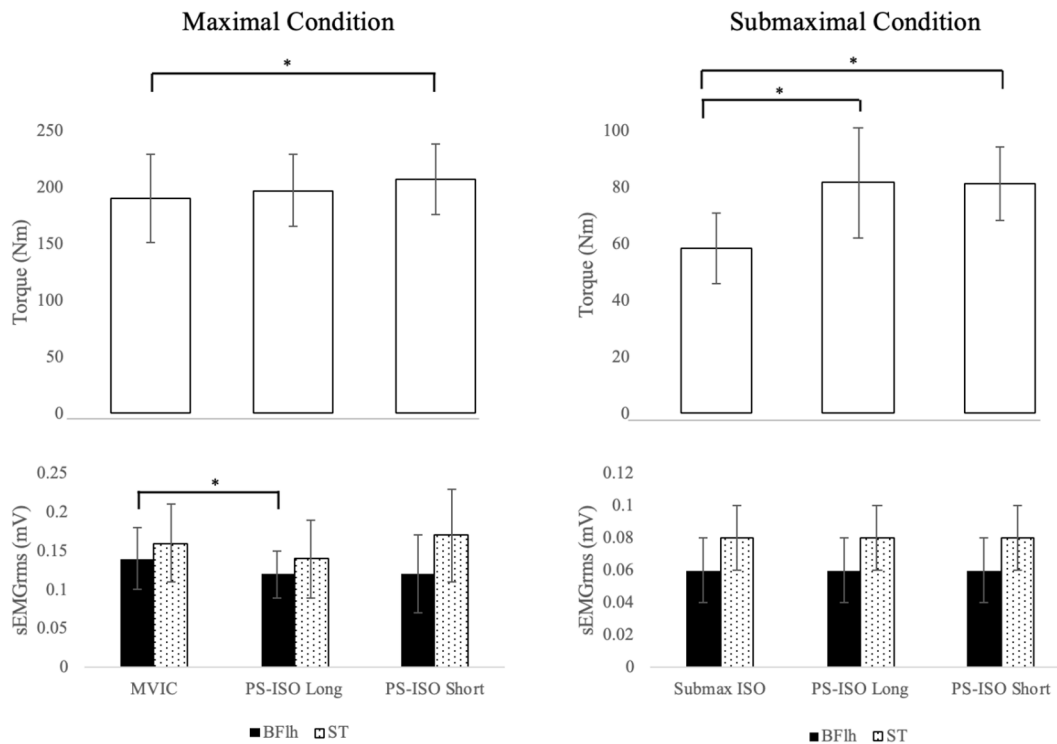
Fig. 3. Baseline and PS-ISO values of knee flexion torque (Nm) and sEMG$_{RMS}$ muscle activation amplitudes (mV) in maximal and submaximal conditions of long (60°) and short (30°) joint rotations. Note: In the PS-ISO$_{SUB-long}$ and PS-ISO$_{SUB-short}$ conditions, participants mediated activation levels to 50%MVIA $\pm$ 10% of sEMG$_{RMS}$. * p = <0.05 indicates a statistically significant difference between baseline and experimental values.

experiment, it must also be acknowledged that other, non-contractile elements may have contributed to these PS-ISO steady-state forces.

4.1. Dynamic MTU behaviour during PS-ISO contractions

This is the first investigation to observe lengthening of the BF*lh* muscle during PS-ISO contractions. This finding is similar to previous findings which confirmed muscle lengthening of the knee extensors (Fukutani et al., 2016) and plantarflexors (Fukutani et al., 2019) during PS-ISO contractions. Confirmation of active muscle lengthening during the PS-ISO contractions leads us to conclude that titin likely contributed to the increased force observed (Fukutani and Herzog, 2019). Relying on direct observations of muscle behaviour during PS-ISO contractions strengthens this conclusion, particularly in light of the sound body of evidence that has demonstrated such a link in *in vitro* experiments (Herzog and Leonard, 2005). Similar to the current study, Fukutani et al. (2016) reported that in maximal voluntary PS-ISO contractions of the knee extensors, the muscle consistently lengthened during the eccentric phase. Previous investigators have reasoned that modulation of muscle lengthening is influenced by muscle-tendon interaction (Farris et al., 2016) or the elimination of slack (Herbert et al., 2015) within the musculotendinous unit during the isometric pre-activation phase. Our findings suggest that these modulations may also be influential during submaximal intensity PS-ISO contractions. Hence the current results support previous evidence that isometric pre-activation is influential in muscle lengthening during maximal and now, submaximal PS-ISO contractions (Fukutani and Herzog, 2019, Fukutani et al., 2019).

The observation of variation in proximo-distal length change of BF*lh* tendons during PS-ISO contractions is new and novel, warranting further

investigation. Proximal and distal tendons behaved independently of each other during PS-ISO contractions in BF*lh*. The proximal tendon was observed to shorten, whilst the distal tendon was observed to lengthen (Fig. 4). We theorise that complex interactions occurring within the musculotendinous unit between the muscle (joint position and variation in moment arm between joints, pennation angle, fascicle length, muscle thickness and variability in proximo-distal fibre arrangement, compartmentalisation and inscription) (Higham and Biewener, 2011, Kellis, 2018) and series elastic element (visco-elastic properties, physiological cross-sectional area and aponeurosis morphology function) (Lersch et al., 2012) contributed to the observed behaviour. However, these suppositions regarding variation in proximo-distal length change are largely speculative due to sparse *in vivo* evidence, particularly concerning BF*lh* (Kellis, 2018). It is, therefore, recommended that further investigation is undertaken into the effect of proximo-distal length change variation in bi-articular muscles during PS-ISO contractions (see Figs. 5 and 6).

4.2. Neuromuscular influences on PS-ISO contractions

The magnitude of rFE during maximal and submaximal conditions (Fig. 3) was greater than the previous investigation of the hamstring muscle group (4–5%) (Shim and Garner, 2012). There is little evidence to suggest that underlying mechanical mechanisms of rFE (i.e. titin stiffness), are solely responsible for the disparity. It is possible that the magnitude of rFE in the maximal conditions, and particularly the PS-ISO$_{MAX-long}$ condition, was influenced by tension mediated factors from peripheral sensory inputs via altered inhibitory sensory feedback to the agonist motor neuron pool (Contento et al., 2020). This sensory
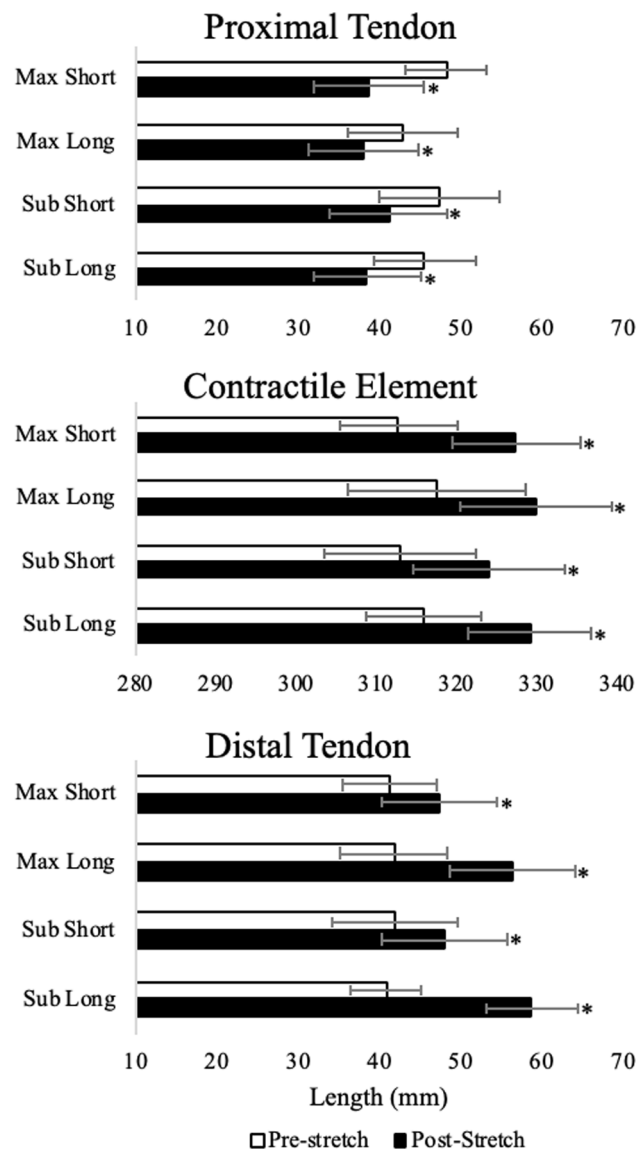
Fig. 4. Whole muscle, proximal and distal tendon lengths, at the start and end of the active-stretch phase of the PS-ISO contractions. Note: PS-ISO$_{MAX-long}$ and PS-ISO$_{SUB-long}$ contractions were of maximal intensity and occurred over a joint excursion of 60° at 60°.s. PS-ISO$_{MAX-short}$ and PS-ISO$_{SUB-short}$ contractions were of submaximal intensity and occurred over a joint excursion of 30° at 60°.s. * p = <0.05 indicates a statistically significant difference between pre-stretch and post-stretch.

feedback can result in reduced muscle activation (Sypkes et al., 2018) (Fig. 3). The BF*lh* muscle is known to be highly prone to musculotendinous injury (Timmins et al., 2015), we propose that the activation reduction may be the result of a protective response within the BF*lh* muscle. It has been suggested that 1b afferent tension mediating factors may provide a protective effect by limiting tension within the musculotendinous unit to reduce the likelihood of musculotendinous injury (Hahn et al., 2012). This protective mechanism might have been more pronounced in the BF*lh* muscle during the PS-ISO$_{MAX-long}$ condition if the response of the Golgi tendon organ was augmented due to a greater joint excursion under higher musculotendinous unit tension (Gregory et al., 2002). As activation reduction was not observed in ST sEMG$_{RMS}$, this

may provide further evidence of the muscle-specific nature of corticospinal excitability (Giesebrecht et al., 2010).

Where tension mediation factors may have reduced rFE in one of the maximal conditions, it is plausible that tension mediated factors may have lesser influence on rFE in submaximal activation matched conditions. Contento et al. (2020) noted that the tension-dependent Golgi tendon organ and the 1b afferent fibres were the most likely contributors in modulating agonist motor neuron excitability during voluntary control of submaximal contractions in the rFE steady-state. The current findings present the possibility that submaximal PS-ISO contractions may result in a relatively greater proportion of rFE. A greater proportion of rFE may be of benefit where elevated force is desirable without
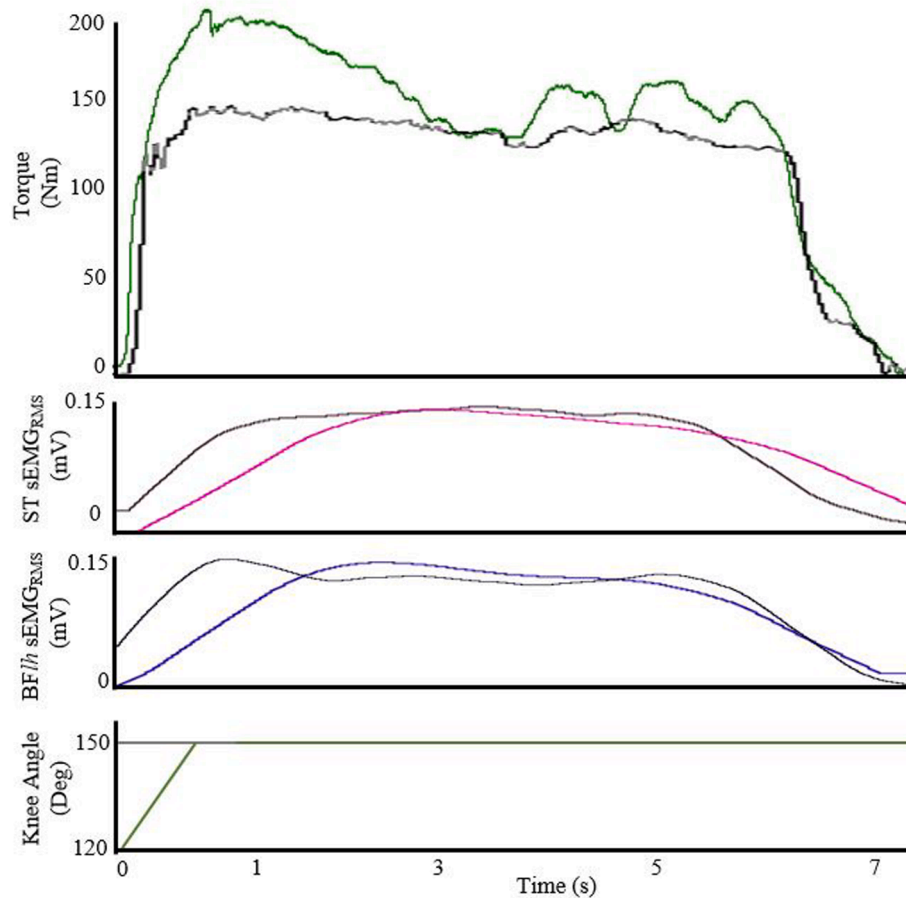
Fig. 5. Torque and muscle activation of biceps femoris long-head (BF*lh*) and semitendinosus (ST) during maximal baseline isometric contractions at 150° knee flexion (180° is equal to full knee extension) (in grey) and post-stretch isometric contractions with a 30° joint rotation at 60°.s^{-1} (in colour).

increased muscle activation. Although currently untested, submaximal PS-ISO contractions in series (as per traditional strength training) may be of benefit in situations such as in injury rehabilitation.

Whilst great care was taken in designing and undertaking this investigation, it should be noted that limitations exist with the collection and interpretation of 2-D ultrasound images of a dynamic muscle contraction moving in a 3-D space, as well as interpretation of sEMG of

the hamstring muscle group where the effect of cross-talk can influence interpretation of sEMG signals.

5. Conclusion

This study provides novel evidence confirming rFE in the knee flexors during maximal and submaximal PS-ISO contractions over two
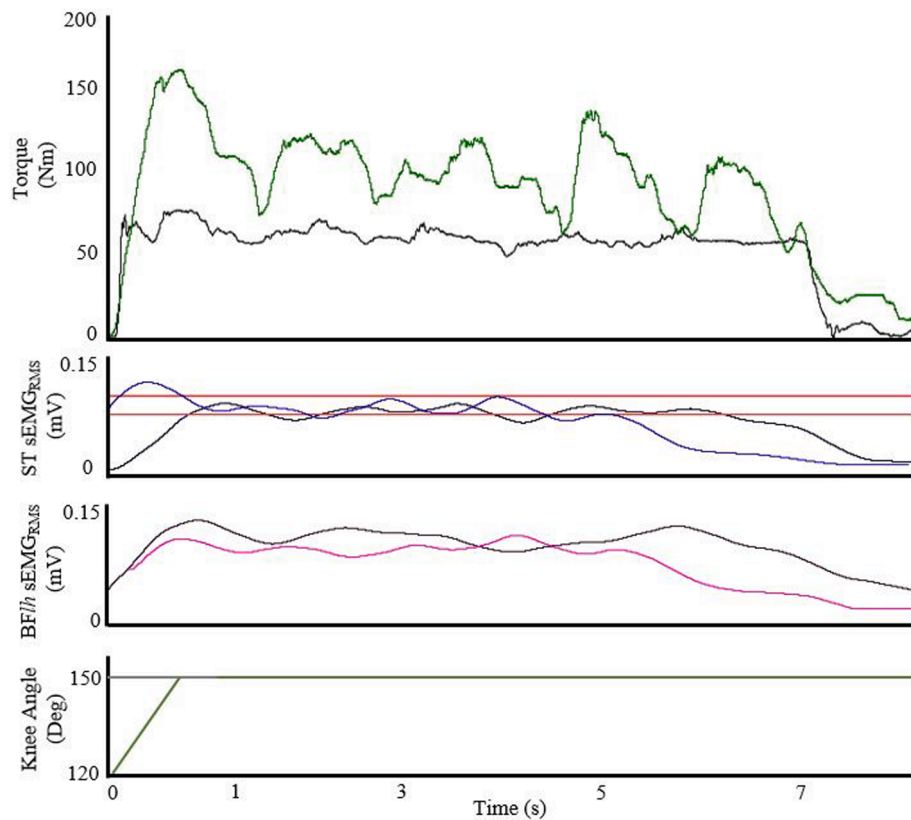
Fig. 6. Torque and muscle activation of biceps femoris long-head (BF*lh*) and semitendinosus (ST) during activation matched submaximal baseline isometric contractions at 150° knee flexion (180° is equal to full knee extension) (in grey) and activation matched submaximal post-stretch isometric contractions with a 30° joint rotation at 60°.s^{-1} (in colour). Semitendinosus activation matching target indicated by red guidelines.

stretch magnitudes. The present study was the first to observe muscle length change in knee flexors during maximal and submaximal PS-ISO contractions. It is also the first to observe proximo-distal length change in any muscle during PS-ISO contractions. We postulate that tension-mediated neuromechanical factors may influence rFE in maximal PS-ISO contractions of the knee flexors. The enhanced isometric steady-state force in submaximal PS-ISO contractions may be of particular interest to those looking to rehabilitate injured muscle, restore strength and minimise excessive scar tissue formation. Future research should investigate potential hypertrophic effect of consecutive bouts of PS-ISO contractions simulating a training stimulus.

Authorship

All listed authors satisfy the criteria for authorship as outlined by the International Committee of Medical Journal Editors.

Declaration of Competing Interest

None.

References

Aeles, J., Lichtwark, G.A., Lenchant, S., Vanlommel, L., Delabastita, T., Vanwanseele, B., 2017. Information from dynamic length changes improves reliability of static ultrasound fascicle length measurements. PeerJ 5, e4164.

Askling, C.M., Nilsson, J., Thorstensson, A., 2010. A new hamstring test to complement the common clinical examination before return to sport after injury. Knee Surg. Sports Traumatol. Arthrosc. 18, 1798–1803.

Askling, C.M., Tengvar, M., Tarassova, O., Thorstensson, A., 2014. Acute hamstring injuries in Swedish elite sprinters and jumpers: a prospective randomised controlled clinical trial comparing two rehabilitation protocols. Br. J. Sports Med. 48, 532–539.

Brockett, C.L., Morgan, D.L., Proske, U., 2001. Human hamstring muscles adapt to eccentric exercise by changing optimum length. Med. Sci. Sports Exerc. 33, 783–790.

Brooks, J.H., Fuller, C.W., Kemp, S.P., Reddin, D.B., 2006. Incidence, risk, and prevention of hamstring muscle injuries in professional rugby union. Am. J. Sports Med. 34, 1297–1306.

Chen, J., Power, G.A., 2019. Modifiability of the history dependence of force through chronic eccentric and concentric biased resistance training. J. Appl. Physiol. 126, 647–657.

COHEN, J. 2013. Statistical Power Analysis for the Behavioral Sciences, Academic press.

Comfort, P., Green, C.M., Matthews, M., 2009. Training considerations after hamstring injury in athletes. Strength Cond. J. 31, 68–74.

Contento, V.S., Dalton, B.H., Power, G.A., 2020. The Inhibitory Tendon-Evoked Reflex Is Increased in the Torque-Enhanced State Following Active Lengthening Compared to a Purely Isometric Contraction. Brain Sci. 10, 13.

Dalton, B.H., Contento, V.S., Power, G.A., 2018. Residual force enhancement during submaximal and maximal effort contractions of the plantar flexors across knee angle. J. Biomech. 78, 70–76.

Edman, K.A., Elzinga, G., Noble, M.I., 1982. Residual force enhancement after stretch of contracting frog single muscle fibers. J. Gen. Physiol. 80, 769–784.

Erickson, L.N., Sherry, M.A., 2017. Rehabilitation and return to sport after hamstring strain injury. J. Sport Health Sci. 6, 262–270.

Farris, D.J., Lichtwark, G.A., Brown, N.A., Cresswell, A.G., 2016. The role of human ankle plantar flexor muscle–tendon interaction and architecture in maximal vertical jumping examined in vivo. J. Exp. Biol. 219, 528–534.

Franchi, M.V., Raiteri, B.J., Longo, S., Sinha, S., Narici, M.V., Csapo, R., 2018. Muscle architecture assessment: strengths, shortcomings and new frontiers of in vivo imaging techniques. Ultrasound Med. Biol. 44, 2492–2504.

Fukutani, A., Herzog, W., 2019. Current Understanding of Residual Force Enhancement: Cross-Bridge Component and Non-Cross-Bridge Component. Int. J. Mol. Sci. 20, 5479.

Fukutani, A., Misaki, J., Isaka, T., 2016. Influence of preactivation on fascicle behavior during eccentric contraction. SpringerPlus 5, 760.

Fukutani, A., Shimoho, K., Isaka, T., 2019. Isometric preactivation before active lengthening increases residual force enhancement. Scand. J. Med. Sci. Sports 29, 1153–1160.

Gabbe, B.J., Bennell, K.L., Finch, C.F., Wajswelner, H., Orchard, J., 2006. Predictors of hamstring injury at the elite level of Australian football. Scand. J. Med. Sci. Sports 16, 7–13.

Gibbs, N., Cross, T., Cameron, M., Houang, M., 2004. The accuracy of MRI in predicting recovery and recurrence of acute grade one hamstring muscle strains within the same season in Australian Rules football players. J. Sci. Med. Sport 7, 248–258.

Giesebrecht, S., Martin, P.G., Gandevia, S.C., Taylor, J.L., 2010. Facilitation and inhibition of tibialis anterior responses to corticospinal stimulation after maximal voluntary contractions. J. Neurophysiol. 103, 1350–1356.

Gregory, J., Brockett, C.L., Morgan, D.L., Whitehead, N.P., Proske, U., 2002. Effect of eccentric muscle contractions on Golgi tendon organ responses to passive and active tension in the cat. J. Physiol. 538, 209–218.

Hahn, D., Hoffman, B.W., Carroll, T.J., Cresswell, A.G., 2012. Cortical and spinal excitability during and after lengthening contractions of the human plantar flexor muscles performed with maximal voluntary effort. PLoS ONE 7, e49907.

Heiderscheit, B.C., Sherry, M.A., Silder, A., Chumanov, E.S., Thelen, D.G., 2010. Hamstring strain injuries: recommendations for diagnosis, rehabilitation, and injury prevention. J. Orthop. Sports Phys. Ther. 40, 67–81.

Herbert, R., Héroux, M., Diong, J., Bilston, L., Gandevia, S., Lichtwark, G., 2015. Changes in the length and three-dimensional orientation of muscle fascicles and aponeuroses with passive length changes in human gastrocnemius muscles. J. Physiol. 593, 441–455.

Hermens, H.J., Freriks, B., Merletti, R., Stegeman, D., Blok, J., Rau, G., Disselhorst-Klug, C., Hägg, G., 1999. European recommendations for surface electromyography. Roessingh Res. Dev. 8, 13–54.

Herzog, W., Leonard, T.R., 2005. The role of passive structures in force enhancement of skeletal muscles following active stretch. J. Biomech. 38, 409–415.

Hickey, J.T., Timmins, R.G., Maniar, N., Rio, E., Hickey, P.F., Pitcher, C.A., Williams, M. D., Opar, D.A., 2020. Pain-Free versus Pain-Threshold rehabilitation following acute hamstring strain injury: a randomized controlled trial. J. Orthopaedic Sports Phys. Therapy 50, 91–103.

Higham, T.E., Biewener, A.A., 2011. Functional and architectural complexity within and between muscles: regional variation and intermuscular force transmission. Philos. Trans. Roy. Soc. B: Biol. Sci. 366, 1477–1487.

Järvinen, T.A., Järvinen, T.L., Kääriäinen, M., Kalimo, H., Järvinen, M., 2005. Muscle injuries: biology and treatment. Am. J. Sports Med. 33, 745–764.

Kellis, E. 2018. Intra-and Inter-Muscular Variations in Hamstring Architecture and Mechanics and Their Implications for Injury: A Narrative Review. Sports Med., 48, 2271-2283.

Kwah, L.K., Pinto, R.Z., Diong, J., Herbert, R.D., 2013. Reliability and validity of ultrasound measurements of muscle fascicle length and pennation in humans: a systematic review. J. Appl. Physiol. 114, 761–769.

Lee, H.D., Herzog, W., 2002. Force enhancement following muscle stretch of electrically stimulated and voluntarily activated human adductor pollicis. J. Physiol. 545, 321–330.

Lersch, C., Grötsch, A., Segesser, B., Koebke, J., Brüggemann, G.-P., Potthast, W., 2012. Influence of calcaneus angle and muscle forces on strain distribution in the human Achilles tendon. Clin. Biomech. 27, 955–961.

Orchard, J., Best, T.M., 2002. The management of muscle strain injuries: an early return versus the risk of recurrence. Clin. J. Sport Med. 12, 3–5.

Proske, U., Morgan, D.L., Brockett, C.L., Percival, P., 2004. Identifying athletes at risk of hamstring strains and how to protect them. Clin. Exp. Pharmacol. Physiol. 31, 546–550.

Seiberl, W., Power, G.A., Hahn, D., 2015. Residual force enhancement in humans: current evidence and unresolved issues. J. Electromyogr. Kinesiol. 25, 571–580.

Shim, J., Garner, B., 2012. Residual force enhancement during voluntary contractions of knee extensors and flexors at short and long muscle lengths. J. Biomech. 45, 913–918.

Sypkes, C.T., Kozlowski, B.J., Grant, J., Bent, L.R., McNeil, C.J., Power, G.A., 2018. The influence of residual force enhancement on spinal and supraspinal excitability. PeerJ 6, e5421.

Tilp, M., Steib, S., Schappacher-Tilp, G., Herzog, W., 2011. Changes in fascicle lengths and pennation angles do not contribute to residual force enhancement/depression in voluntary contractions. J. Appl. Biomech. 27, 64–73.

Timmins, R. G., Bourne, M. N., Shield, A. J., Williams, M. D., Lorenzen, C. & Opar, D. A. 2015. Short biceps femoris fascicles and eccentric knee flexor weakness increase the risk of hamstring injury in elite football (soccer): a prospective cohort study. Brit. J. Sports Med., bjsports-2015-095362.

Tyler, T., Schmitt, B., Nicholas, S., McHugh, M., 2015. Rehabilitation After Hamstring Strain Injury Emphasizing Eccentric Strengthening at Long Muscle Lengths: Results of Long Term Follow-up. J. Sport Rehabilit.

Van Der Horst, N., Thorborg, K. & Opar, D. 2020. Hamstring Injury Prevention and Implementation. Prevention and Rehabilitation of Hamstring Injuries. Springer.

van Hooren, B., Bosch, F., 2017a. Is there really an eccentric action of the hamstrings during the swing phase of high-speed running? Part I: a critical review of the literature. J. Sports Sci. 35, 2313–2321.

van Hooren, B., Bosch, F., 2017b. Is there really an eccentric action of the hamstrings during the swing phase of high-speed running? Part II: Implications for exercise. J. Sports Sci. 35, 2322–2333.

Neil Chapman is an accredited clinical exercise physiologist and PhD candidate in Sport and Exercise Science at Southern Cross University, Australia.

Dr. John Whitting is a senior lecturer in biomechanics and kinesiology at Southern Cross University, Australia.

Dr. Suzanne Broadbent is an Associate Professor in Clinical Exercise Physiology at the University of the Sunshine Coast, Australia

Dr. Zac Crowley-McHattan is a lecturer in motor control and motor learning at Southern Cross University, Australia.

Dr. Rudi Meir is an Associate Professor in Strength and Conditioning at Southern Cross University, Australia.